Inorganic Chemistry

Article

pubs.acs.org/IC

Terms of Use

Transmetalation of Aqueous Inorganic Clusters: A Useful Route to the Synthesis of Heterometallic Aluminum and Indium Hydroxo—Aquo Clusters

Maisha K. Kamunde-Devonish,[†] Milton N. Jackson, Jr.,[†] Zachary L. Mensinger,[†,§] Lev N. Zakharov,[‡] and Darren W. Johnson*[,†]

[†]Department of Chemistry & Biochemistry and Materials Science Institute, University of Oregon, Eugene, Oregon 97403-1253, United States

[‡]Center for Advanced Materials Characterization in Oregon (CAMCOR), University of Oregon, Eugene, Oregon 97403-1443, United States

Supporting Information

ABSTRACT: $[Al_xIn_y(\mu_3\text{-}OH)_6(\mu\text{-}OH)_{18}(H_2O)_{24}](NO_3)_{15}$ hydroxy—aquo clusters ($\mathbf{Al_xIn_{13-x}}$) are synthesized through the evaporation of stoichiometrically varied solutions of $\mathbf{Al_{13}}$ and $In(NO_3)_3$ using a transmetalation reaction. Several spectroscopic techniques (^{1}H NMR, ^{1}H-diffusion ordered spectroscopy, dynamic light scattering, and Raman) are used to compare $\mathbf{Al_xIn_{13-x}}$ to its $\mathbf{Al_{13}}$ counterpart. A thin film of aluminum indium oxide was prepared from an $\mathbf{Al_7In_6}$ cluster ink, showing its utility as a precursor for materials.

INTRODUCTION

Transparent electronics and devices have emerged as one of the most promising developments for next-generation technologies. Solution-processed multicomponent materials such as indium gallium oxide (IGO) and aluminum indium oxide (AIO) offer routes to enable new or enhanced performance levels in large area electronics and energy devices such as flat-panel displays, solar cells, and LEDs.[1−6] Here we present a transmetalation process that yields the new hydroxy—aquo cluster $[Al_7In_6(\mu_3\text{-}OH)_6(\mu\text{-}OH)_{18}(H_2O)_{24}](NO_3)_{15}$ ($\mathbf{Al_7In_6}$) (Figure 1) by direct treatment of the related $\mathbf{Al_{13}}$ cluster with indium nitrate. To the best of our knowledge this is the first instance of direct transmetalation of metal ions into the exterior shell of such hydroxy—aquo cluster species. We show that this route not only enables the synthesis of previously reported heterometallic Ga/In clusters, but is the most reliable route to form Al/In congeners.

We have reported the synthetic route to an array of nanoscale Group 13 tridecameric hydroxy—aquo clusters composed of gallium and indium.[7,8] The utility of these clusters as precursors/inks for metal oxide semiconductors was previously demonstrated in an IGO thin film device formed from $\mathbf{Ga_7In_6}$.[8] The resulting dense, uniform, and pinhole-free film represents an emergent example of low-temperature solution processing of thin film transistors (TFTs) in which a completely inorganic cluster was used as a precursor material. This process provides a low-temperature alternative for producing thin films as compared to the deposition and sputtering techniques traditionally used to create similar devices.[6] As a result, we began to explore the use of other inorganic aqueous precursor solutions for materials applications.

Aluminum-containing materials in particular show promise as precursor candidates in several applications including dielectric layers and capacitors.[9−13] However, the current number of soluble, dynamic precursors for low-temperature aqueous processing is limited to $[Al_{13}(\mu_3\text{-}OH)_6(\mu\text{-}OH)_{18}(H_2O)_{24}](NO_3)_{15}$ ($\mathbf{Al_{13}}$),[13−15] $[Al_8(OH)_{14}(H_2O)_{18}](SO_4)_5\cdot 16H_2O$ ($\mathbf{Al_8}$),[16] and $[Al_4(OH)_6(H_2O)_{12}][Al(H_2O)_6]_2(Br_{12})$ ($\mathbf{Al_4}$).[17,18] The synthesis of $\mathbf{Al_{13}}$ originally required the addition of a base (NaOH or NH_4OH) and the carcinogenic additive dibutylnitrosoamine (DBNA).[14] In the case of the heterometallic Al/In clusters, the product was difficult to reproduce under the same conditions. Transmetalation eliminates the need for base and organic reagents and provides a reliable synthesis for preparing these otherwise inaccessible heterometallic clusters, in particular $\mathbf{Al_7In_6}$. Furthermore, we show that the resulting clusters can be used as precursors for smooth, amorphous aluminum indium oxide (AIO) thin films that are comparable to films of similar content produced by atomic layer deposition or sputtering deposition.[9,10,19] In addition, transmetalation is an unusual reaction for aqueous coordination clusters.

Received: December 20, 2013
Published: April 18, 2014

   dx.doi.org/10.1021/ic403121r | Inorg. Chem. 2014, 53, 7101−7105

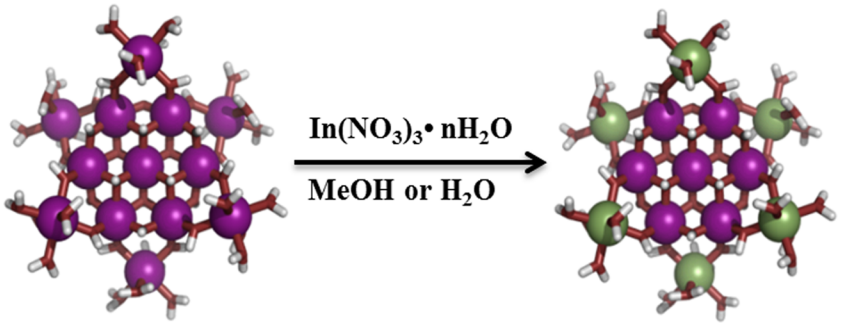

Figure 1. Simple representation of the transformation from Al_{13} to Al_7In_6 upon addition of $In(NO_3)_3$. In^{3+} ions (green) displace Al^{3+} ions (purple) on the labile outer shell of the cluster. Images are wireframe and ball structures generated from the crystal structures of Al_{13} and Al_7In_6.

The metal-exchange phenomenon has been exhibited in several examples of polyoxometalate structures.[20−23] Electrospray ionization mass spectroscopy (ESI-MS) characterization was used to identify mixed-metal phosphate-centered Keggin ions in aqueous tungsten and phosphododecametalate solutions.[20,21] Similar experiments for niobate/tantalate[22] and Mo/V−selenite[23] systems showed additional mixed-metal species. Altering the pH conditions of monomeric salt solutions has led to the substitution of the central metal ion of Keggin Al_{13} by Ga, Fe, or Ge as well as a variety of di- and trivalent metal ions into the Anderson cluster $[Mo_7O_{24}]^{6-}$.[24−29] We explored the potential for metal exchange in tridecameric clusters and discovered that such a process occurs when mixing Al_{13} and $In(NO_3)_3$. As a result indium ions substitute into the exterior metal sites of the cluster to produce Al_7In_6 (Figure 1). The ability of Al_{13} to easily convert into Al_7In_6 hints at dynamic metal and ligand exchange that might occur in solution and influence speciation of Al_{13} and related Al clusters.

While this report focuses on the Al derivatives,[30] related studies reveal that the previously described Ga_7In_6 cluster[8] can also been synthesized via transmetalation. For example, a 1:12 ratio of Ga_{13}/$In(NO_3)_3$ produces Ga_7In_6 (see Experimental Section). The reverse reaction is also possible: when excess $Ga(NO_3)_3$ is added to Ga_7In_6, Ga_{13} forms. This provides further evidence of a dynamic equilibrium between the M_{13} (M = Al or Ga) cluster and $M(NO_3)_3$ monomer. Nuclear magnetic resonance (NMR) spectroscopy, diffusion ordered spectroscopy (^{1}H-DOSY), dynamic light scattering (DLS), and Raman spectroscopy have been used to provide valuable information in the characterization of these inorganic cluster species.[31−33] We have specifically used these techniques in tandem to identify size and structural differences between Al_{13} and Al_7In_6 in solution.

EXPERIMENTAL SECTION

General Methods. All reagents were purchased from commercial sources and were used as received. Aluminum nitrate nonahydrate (99.0% Al), indium nitrate hydrate (99.999% In), and gallium nitrate hydrate (99.99% Ga) were purchased from Strem Chemicals. Methanol (MeOH) was used as received. Unless specified otherwise, all reactions were conducted in standard 20 mL scintillation vials. ^{1}H NMR and ^{1}H-DOSY spectra were obtained on a Varian INOVA-500 MHz NMR Spectrometer. The bipolar pulse pair stimulated echo (Dbppste) pulse sequences were used to acquire diffusion data with a 50 ms diffusion delay, 200 ms gradient length, 20 gradient levels, and nt = 16 scans. The Varian DOSY package was used for processing and measuring the diffusion coefficient (D_t). The hydrodynamic radius (R_h) was calculated using the Einstein−Stokes equation ($R_h = K_bT/6\pi\eta D_t$) where K_b = the Boltzmann constant, T = temperature in kelvin, η = viscosity, and D_t = translational diffusion coefficient.[31] Percent error was calculated using measured values for ferrocene in dimethylsulfoxide (DMSO).[34,35] DLS measurements were taken using the Mobiuζ from Wyatt technologies. The samples were filtered using a 0.1 μm polytetrafluoroethylene (PTFE) syringe tip to remove any particulate matter followed by immediate analysis (t < 1 min). Dynamics software was used and averaged over 20 measurements with a 5 s integration time per acquisition. Raman spectra of the Al_7In_6 single crystals were collected using an Alpha 300S SNOM confocal Raman microscope. The spectra from each sample were averaged over 2000 accumulations at 0.5 s exposure time per scan. Thin films were fabricated via spin coating (3000 rpm for 30 s) a 0.2 M aqueous solution of Al_7In_6 onto a p-type Si wafer pretreated with a piranha solution (7:3 v/v ratio of concentrated H_2SO_4 and 35% H_2O_2). Prior to spin coating, the solutions were filtered through a 0.1 μm PTFE syringe tip to remove any particulate matter and/or potential agglomerates. The subsequent films were then annealed at 300 °C for 30 min prior to analysis.

General Procedure for the Synthesis of Al_7In_6 and Ga_7In_6. A solution of Al_{13} (0.078 g, 0.037 mmol)[14b] and $In(NO_3)_3$ (0.27 g, 0.90 mmol) in MeOH (10 mL) was left open to air to evaporate. After several days crystals of Al_7In_6 formed (10% product yield with respect to starting amount of Al_{13}). Single-crystal X-ray diffraction reveals a structure identical in geometry to the previously reported heterometallic clusters.[8] Ga_7In_6 was synthesized following the same method as for Al_7In_6. A solution of Ga_{13} (0.100 g, 0.037 mmol) and $In(NO_3)_3$ (0.27 g, 0.90 mmol) in MeOH (10 mL) was left open to air to evaporate. Ga_7In_6 crystals formed after several days (20% yield with respect to the amount of Ga_{13}). Both Al_{13} and Ga_{13} were used as is following a wash with acetone. See Electronic Supporting Information for specific spectral details.

RESULTS AND DISCUSSION

The ^{1}H NMR spectra of Al_{13} and Al_7In_6 reveal several differences between the compounds (Figure 2). The peaks between 9.10 and 9.32 ppm in Al_{13} (A) that are indicative of $Al(NO_3)_3$ (inset, C) are mostly absent from B. It appears that the species present in the ^{1}H NMR spectrum of $Al(NO_3)_3$ remains once the crystallization of Al_{13} occurs. Subsequent recrystallization to produce Al_7In_6 removes this species. Another set of peaks is observed between 7.04 and 7.21 ppm. The observed 1:1:1 triplet is associated with a spin one-half nucleus (such as ^{1}H) coupling to an S = 1 nucleus (such as ^{14}N). Al_{13} is produced by the reduction of $Al(NO_3)_3$ by zinc powder.[14] The reduction of nitrate ions by zinc metal is thermodynamically feasible (eqs 1−3), particularly in acidic environments.[36] Therefore, it seems reasonable that the triplet is a result of that reduction process of nitrate to ammonium at an acidic pH. Again, as a consequence of recrystallization, those peaks disappear when Al_7In_6 is formed and isolated.

dx.doi.org/10.1021/ic403121r | Inorg. Chem. 2014, 53, 7101−7105

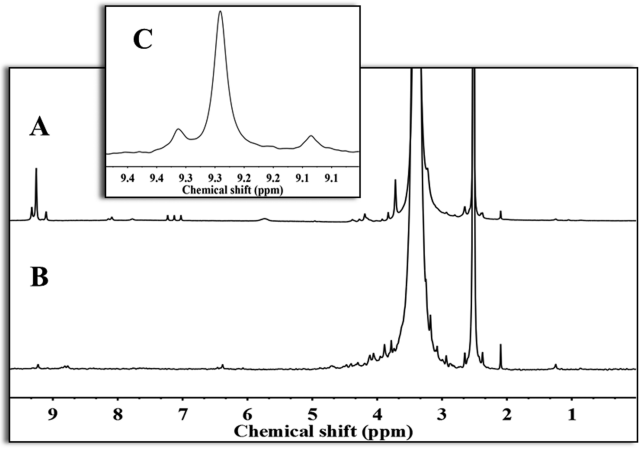

Figure 2. ^{1}H NMR of $\mathbf{Al_{13}}$ (A), $\mathbf{Al_7In_6}$ (B), and $Al(NO_3)_3$ (C). Crystals of $\mathbf{Al_{13}}$ (confirmed using single-crystal XRD) were used for ^{1}H NMR spectroscopic characterization.

$$NO_3^- + 10H^+ + 8e^+ \rightarrow NH_4^+ + 3H_2O \quad E^\circ = +0.88 \tag{1}$$

$$Zn \rightarrow Zn^{2+} + 2e^- \quad E^\circ = -0.76 \tag{2}$$

$$NO_3^- + 10H^+ + 4Zn \rightarrow 4Zn^{2+} + NH_4^+ + 3H_2O \quad E^\circ = +2.16 \tag{3}$$

^{1}H-DOSY was performed to compare the sizes of $\mathbf{Al_{13}}$ and $\mathbf{Al_7In_6}$ in solution. The R_h of $\mathbf{Al_{13}}$ and $\mathbf{Al_7In_6}$ were essentially equivalent (R_h = 1.1 ± 0.3 nm and 1.0 ± 0.3 nm, respectively) in DMSO-d_6 although we expected the R_h for $\mathbf{Al_7In_6}$ to be slightly larger than that of $\mathbf{Al_{13}}$ based upon the size of the atomic radii for Al (1.431 Å) and In (1.65 ± 0.03 Å)[37] and the average calculated Al−O (1.839 Å) and In−O (2.086 Å) bond lengths.

Utilizing DLS as a corroborative technique to DOSY, we also determined the size of both the $\mathbf{Al_{13}}$ and $\mathbf{Al_7In_6}$ clusters in DMSO-d_6 as well as in aqueous solutions. In a direct solvent comparison with the DOSY experiment, the R_h of $\mathbf{Al_{13}}$ and $\mathbf{Al_7In_6}$ in DMSO-d_6 is very close to that measured with DOSY at 1.0 ± 0.3 nm and 0.9 ± 0.4 nm, respectively (Figure 3). In water, DLS shows that the $\mathbf{Al_{13}}$ cluster is 1.0 ± 0.1 nm (Figure 3). By comparison, the measured R_h for $\mathbf{Al_7In_6}$ is 15.7 ± 2.0 nm, roughly an order of magnitude larger in water than its homometallic counterpart, suggesting that the discrete $\mathbf{Al_7In_6}$ cluster is not a stable species in water but rather aggregates favoring the formation of larger, apparently stable nanoparticles.

The R_h of $\mathbf{Al_{13}}$ in water is the same as in DMSO-d_6, suggesting the cluster is stable in both solvents. However, the autocorrelation function suggests higher polydispersity for the cluster in DMSO-d_6 than in H_2O. This difference is likely due to the viscosity effects of DMSO-d_6 (2.0 cP vs 0.89 cP for DMSO and H_2O, respectively, at 25 °C) that would cause fluctuations in cluster rates of diffusion in solution. Solution studies are currently in progress to fully understand the solution speciation and other dynamic characteristics of these clusters in various solvents. Nevertheless, it is clear that the two clusters behave differently in aqueous solution and these techniques can provide a routine platform for understanding the solution chemistry of hydroxo-aquo clusters in general.

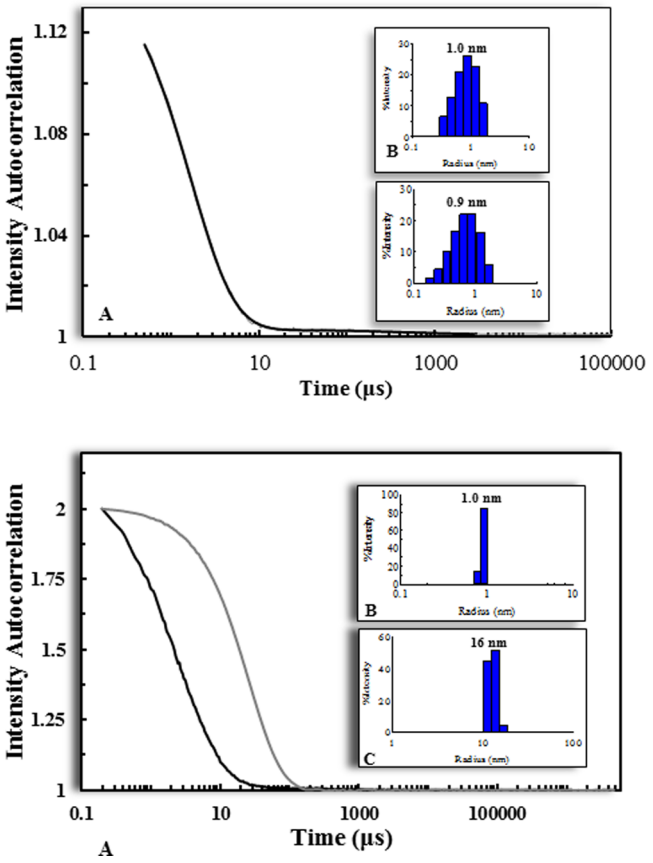

Figure 3. (top) (A) Autocorrelation function of 2 mM $\mathbf{Al_{13}}$ (black) and 2 mM $\mathbf{Al_7In_6}$ (gray) in DMSO-d_6 (traces stack on top of each other). Hydrodynamic radii of $\mathbf{Al_{13}}$ (B) and $\mathbf{Al_7In_6}$ (C) in DMSO-d_6 are displayed in the insets. (bottom) (A) Autocorrelation function of 0.2 M $\mathbf{Al_{13}}$ (black) and 0.2 M $\mathbf{Al_7In_6}$ (gray) in H_2O. Hydrodynamic radii of $\mathbf{Al_{13}}$ (B) and $\mathbf{Al_7In_6}$ (C) in H_2O are displayed in the insets.

Solid-state Raman spectroscopy is a valuable technique for characterizing single crystals of this cluster type. In previous work, quantum mechanical computations were used to identify the various vibrational modes associated with $\mathbf{Al_{13}}$.[33] Upon investigation of $\mathbf{Al_7In_6}$, the incorporation of indium into the cluster changes the vibrational features of the cluster, and therefore each cluster has its own unique Raman signature (Figure 4).

The spectrum of $\mathbf{Al_7In_6}$ reveals several new modes that distinguish it from $\mathbf{Al_{13}}$ (Figure 4). The most significant difference between the two clusters is the disappearance of the breathing mode of $\mathbf{Al_{13}}$ at 478 cm^{-1} in the spectrum for $\mathbf{Al_7In_6}$. The broad peak with medium relative intensity at 428 cm^{-1} can be attributed to Al−OH−In stretching vibrations. A narrower band with slightly less intensity at 374 cm^{-1} corresponds to the vibrations of In and the coordinated waters (In−OH_2) of the exterior cluster shell. The lower wavenumber peak at 212 cm^{-1} can be also be assigned as an In−O bending mode due to the lack of spectral evidence for a bound nitrate to the cluster.[38] More specifically, there are no signs of peak splitting in the antisymmetric and symmetric NO_3^- peaks (720 and 1048 cm^{-1}, respectively) that denote the existence of an indium nitrato species ($In(NO_3)(H_2O)_5^{2+}$).[38] The vibrational modes typically associated with the free NO_3^- ions in $\mathbf{Al_7In_6}$ are consistent with those observed in $\mathbf{Al_{13}}$ (721 cm^{-1}, 1048 cm^{-1}, 1350 cm^{-1}, and 1411 cm^{-1}) suggesting that the nitrates behave

dx.doi.org/10.1021/ic403121r | Inorg. Chem. 2014, 53, 7101−7105

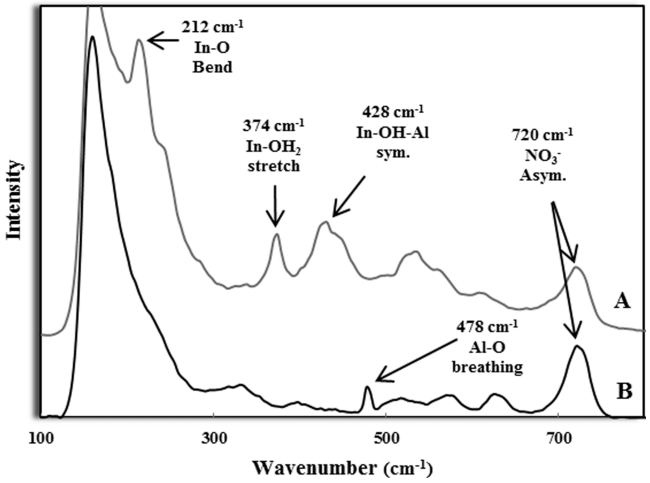

Figure 4. Solid-state Raman spectra of Al_{13} (black) and Al_7In_6 (gray) between 100 and 800 cm^{-1}.

similarly in the two clusters. There are also several weaker modes present between 450 and 650 cm^{-1} that are attributed to the Al−O vibrations, similar to what has been previously reported for Al_{13}.[33]

Thin films were prepared as a single layer from an aqueous solution at 0.2 M total metal concentration of the Al_7In_6 cluster. Both transmission electron microscopy (TEM) and X-ray reflectivity (XRR) measurements show a film thickness of close to 6 nm (5.7 nm for scanning electron microscopy (SEM) and 5.5 ± 0.2 nm for XRR). TEM and atomic force microscopy (AFM) images reveal that Al_7In_6 produces uniform and atomically smooth thin films from spin-coating when used as a solution precursor (Figure 5). As compared to the IGO solution-processed film formed from Ga_7In_6, we see with TEM that the AIO film surface morphology is also dense and pinhole-free with minimal signs of inhomogeneity.[8] The 16 μm^2 AFM image shows that the Al_7In_6 film is very smooth across the surface (root mean square (RMS) roughness = 0.145 nm), despite film thinness. Energy dispersive X-ray spectroscopy (EDX) analysis confirms the existence of an oxide composed of Al and In in the film (aluminum indium oxide, AIO). The relative composition measurements show a ratio of $Al_{1.02}In_{0.98}O_{2.95}$, close in comparison to the aforementioned IGO thin-film device.[8] Device performance and applications will be reported in due course.

CONCLUSION

In summary, we were able to synthesize the heterometallic Al_7In_6 hydroxo−aquo cluster via a transmetalation reaction. ^1H NMR and Raman spectroscopies reveal that in the solution and solid states, respectively, the Al_7In_6 cluster has distinct spectral features in relation to the Al_{13} cluster. ^1H-DOSY and DLS show that these clusters persist in solution as multiple discrete species. In addition a dense, smooth, uniform, thin film of AIO was fabricated using Al_7In_6. By utilizing these techniques to identify Al_7In_6 in the solid and solution phases, we are better equipped to explore and understand the complex solution dynamics and exchange reactions of these clusters. These clusters also serve as potential precursors for solution deposition of metal−oxide thin films. Heterometallic clusters also provide the additional advantage of tuning the metal ratios at the molecular level in spin-coating applications.

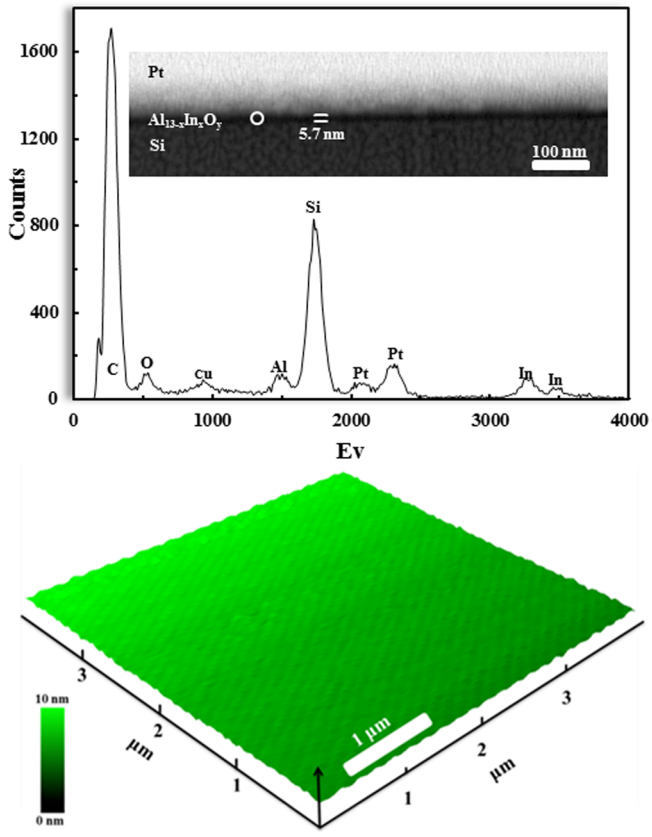

Figure 5. (top) EDX analysis of the solution-processed Al_7In_6 precursor and cross-sectional TEM (top insert) of the $Al_{13-x}In_xO_y$ thin film. The white circle represents the spot on which the EDX scan was performed. (bottom) AFM three-dimensional side view of $Al_{13-x}In_xO_y$ thin film (16 μm^2).

ASSOCIATED CONTENT

Supporting Information

Detailed experimental section that includes synthesis and characterization techniques. Crystallographic data for Al_7In_6 in CIF format. Full Raman spectra of solid-state samples of Al_{13}, Al_7In_6, and $In(NO_3)_3$. Raman peak assignments of the Al_7In_6 material. DLS data log sheets for Al_{13} and Al_7In_6 clusters in DMSO and H_2O. This material is available free of charge via the Internet at http://pubs.acs.org.

AUTHOR INFORMATION

Corresponding Author

*E-mail: dwj@uoregon.edu.

Present Address

[§]Division of Science and Mathematics, University of Minnesota Morris, Morris, MN 56267

Author Contributions

The manuscript was written through contributions of all authors. All authors have given approval to the final version of the manuscript. M.K.K.-D. and M.N.J., Jr. contributed equally to this work.

Funding

This work was generously supported by the NSF Center for Sustainable Materials Chemistry (CHE-1102637). University of Oregon NMR facilities are supported by NSF CHE-0923589. D.W.J. is a Scialog Fellow of Research Corporation for Science Advancement.

Notes

The authors declare no competing financial interest.

■ ACKNOWLEDGMENTS

The authors would like to thank Joshua Razink in the University of Oregon CAMCOR facility for assistance with TEM film imaging. We gratefully acknowledge the use of CAMCOR facilities, which were purchased with a combination of federal and state funding.

■ REFERENCES

(1) Anderson, J. T.; Munsee, C. L.; Hung, C. M.; Phung, T. M.; Herman, G. S.; Johnson, D. C.; Wager, J. F.; Keszler, D. A. *Adv. Funct. Mater.* **2007**, *17*, 2117−2124.
(2) Meyers, S. T.; Anderson, J. T.; Hong, D.; Hung, C. M.; Wager, J. F.; Keszler, D. A. *Chem. Mater.* **2007**, *19*, 4023−4029.
(3) Keszler, D. A. *Nat. Mater.* **2011**, *10*, 9−10.
(4) Wager, J. F.; Yeh, B.; Hoffman, R. L.; Keszler, D. A. *Curr. Opin. Solid State Mater. Sci.* **2014**, *in press*, http://dx.doi.org/10.1016/j.cossms.2013.07.002.
(5) Mitzi, D. *Solution Processing of Inorganic Materials;* John Wiley & Sons: Hoboken, NJ, 2009.
(6) (a) Presley, R. A.; Hong, D.; Chiang, H. Q.; Hung, C. M.; Hoffman, R. L.; Wager, J. F. *Solid-State Electron.* **2006**, *50*, 500−503. (b) Bloor, L. G.; Carmalt, C. J.; Pugh, D. *Coord. Chem. Rev.* **2011**, *255*, 1293−1318.
(7) Rather, E.; Gatlin, J. T.; Nixon, P. G.; Tsukamoto, T.; Kravtsov, V.; Johnson, D. W. *J. Am. Chem. Soc.* **2005**, *127*, 3242−3243.
(8) Mensinger, Z. L.; Gatlin, J. T.; Meyers, S. T.; Zakharov, L. N.; Keszler, D. A.; Johnson, D. W. *Angew. Chem., Int. Ed.* **2008**, *47*, 9484−9486.
(9) Hwang, Y. H.; Jeon, J. H.; Seo, S. J.; Bae, B. S. *Electrochem. Solid-State Lett.* **2009**, *12*, 336−339.
(10) Hwang, Y. H.; Bae, B. S. *J. Disp. Technol.* **2013**, *9*, 704−709.
(11) Kim, H. J.; No, S. Y.; Eom, D.; Hwang, C. S. *J. Korean Phys. Soc.* **2006**, *49*, 1271−1275.
(12) Silva, R.; Zaniquelli, M. E. D. *Thin Solid Films* **2004**, *449*, 86−93.
(13) Fan, G.; Sun, W.; Wang, H.; Feng, L. *Chem. Eng. J.* **2011**, *174*, 467−473.
(14) (a) Gatlin, J. T.; Mensinger, Z. L.; Zakharov, L. N.; MacInnes, D.; Johnson, D. W. *Inorg. Chem.* **2008**, *47*, 1267. (b) Wang, W.; Wentz, K. M.; Hayes, S. E.; Johnson, D. W.; Keszler, D. A. *Inorg. Chem.* **2011**, *50*, 4683−4685.
(15) Al_{13} also synthesized with the Cl^- counteranion: Sun, Z.; Zhao, H. D.; Tong, H. G. E.; Wang, R. F.; Zhu, F. Z. *Chin. J. Struct. Chem.* **2006**, *25*, 1217−1227.
(16) Casey, W. H.; Olmstead, M. M.; Phillips, B. L. *Inorg. Chem.* **2005**, *44*, 4888−4890.
(17) Sun, Z.; Wang, H.; Feng, H.; Zhang, Y.; Du, S. *Inorg. Chem.* **2011**, *50*, 9238−9242.
(18) Mensinger, Z. L.; Wang, W.; Keszler, D. A.; Johnson, D. W. *Chem. Soc. Rev.* **2012**, *41*, 1019−1030.
(19) Socol, G.; Socol, M.; Stefan, N.; Axente, E.; Popecsu-Pelin, G.; Craciun, D.; Duta, L.; Mihailescu, C. N.; Mihailescu, I. N.; Stanculesu, A.; Visan, D.; Sava, V.; Galca, A. C.; Luculescu, C. R.; Craciun, V. *Appl. Surf. Sci.* **2012**, *260*, 42−46.
(20) Deery, M. J.; Howarth, O. W.; Jennings, K. R. *J. Chem. Soc., Dalton Trans.* **1997**, 4783−4788.
(21) Spyratou, A.; Clifford, S.; Melich, X.; Deville, C.; Tissot, M.; Bonvin, G.; Perrottet, P.; Williams, A. *Aust. J. Chem.* **2009**, *62*, 1291−1299.
(22) Sahureka, F.; Burns, R. C.; Nagy-Felsobuki, E. I. *Inorg. Chim. Acta* **2003**, *351*, 69−78.
(23) Corella-Ochoa, M. N.; Miras, H. N.; Long, D. L.; Cronin, L. *Chem.—Eur. J.* **2012**, *18*, 13743−13754.
(24) Lee, A. P.; Phillips, B. L.; Olmstead, M. M.; Casey, W. H. *Inorg. Chem.* **2001**, *40*, 4485−4487.
(25) Lee, A. P.; Furrer, G.; Casey, W. H. *J. Colloid Interface Sci.* **2002**, *250*, 269−270.
(26) Parker, W. O., Jr.; Millini, R.; Kiricsi, I. *Inorg. Chem.* **1997**, *36*, 571−575.
(27) Keggin, J. F. *Proc. R. Soc. Lond. A* **1934**, *144*, 75−100.
(28) In a rare related counterexample (of an oxo/hydroxo cluster rather than a hydroxo/aquo cluster), we previously showed that an Anderson molybdate could undergo a central metal substitution during the crystallization process. In this structural paper we did not demonstrate cluster-to-cluster transmetalation in solution: Mensinger, Z. L.; Zakharov, L. N.; Johnson, D. W. *Acta Crystallogr. Sect. E: Struct. Rep. Online* **2008**, *E64*, i8−i9.
(29) Gili, P.; Nunez, P.; Lorenzo-Luis, P. A. *Acta Crystallogr., Sect. C: Cryst. Struct. Commun.* **2006**, *56*, E441−E442.
(30) To date $Al_{13-x}In_x$ clusters $Al_{10}In_3$ and Al_8In_5 have also been synthesized via transmetalation.
(31) Oliveri, A. F.; Carnes, M. E.; Baseman, M. M.; Johnson, D. W. *Angew. Chem., Int. Ed.* **2012**, *51*, 10992−10996.
(32) Oliveri, A. F.; Elliott, E. W.; Carnes, M. E.; Hutchison, J. E.; Johnson, D. W. *ChemPhysChem* **2013**, *14*, 2655−2661.
(33) Jackson, M. N. J., Jr; Willis, L. A.; Chang, I.-Y.; Carnes, M. E.; Scatena, L.; Cheong, P. H.-Y.; Johnson, D. W. *Inorg. Chem.* **2013**, *52*, 6187−6192.
(34) Vorotyntsev, M. A.; Zinovyeva, V. A.; Picquet, M. *Electrochim. Acta* **2010**, *55*, 5063−5070.
(35) Tsierkezos, N. G. *J. Solution Chem.* **2007**, *36*, 289−302.
(36) Cheng, I. F.; Muftikian, R.; Fernando, Q.; Korte, N. *Chemosphere* **1997**, *35*, 2689−2695.
(37) Aldridge, S.; Downs, A. J. *The Group 13 Metals Aluminum, Gallium, Indium, and Thallium: Chemical Patterns and Peculiarities;* John Wiley & Son, Ltd.: London, U.K., 2011.
(38) Rudolph, W. W.; Fischer, D.; Tomney, M. R.; Pye, C. C. *Phys. Chem. Chem. Phys.* **2004**, *6*, 5145−5155.